

Copernicus Global Land Operations

“Vegetation and Energy”

”CGLOPS-1”

Framework Service Contract N° 199494 (JRC)

ALGORITHM THEORETICAL BASIS DOCUMENT

SURFACE ALBEDO

COLLECTION 1KM

VERSION 1

Issue 2.11

Organization name of lead contractor for this deliverable: METEO-France

Book Captain: Dominique Carrer (METEO-France)

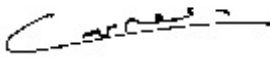

Contributing Authors: Bruno Smets (VITO)

Xavier Ceamanos (METEO-France)

Jean-Louis Roujean (former METEO-France)

Dissemination Level		
PU	Public	X
PP	Restricted to other programme participants (including the Commission Services)	
RE	Restricted to a group specified by the consortium (including the Commission Services)	
CO	Confidential, only for members of the consortium (including the Commission Services)	

Document Release Sheet

Book captain:	Dominique Carrer	Sign 	Date 05.02.2018
Approval:	Roselyne Lacaze	Sign 	Date 05.02.2018
Endorsement:	Michael Cherlet	Sign	Date
Distribution:	Public		

Change Record

Issue/Rev	Date	Page(s)	Description of Change	Release
	28.03.2013	All	Geoland2 document, Issue I1.20, 19.12.2011	I1.00
I1.00	10.09.2014	All	Move geoland2 document to Global Land service document	I1.01
I1.01	26.01.2015	16-17; 26	Adaptation to PROBA-V products	I2.00
I2.00	08.12.2017	16-17	Updated section "Input Data" to be conform to updated TOC-r product, support both SPOT-VGT and PROBA-V	I2.10
I2.10	05.02.2018	16, 32	Update references	I2.11

TABLE OF CONTENTS

Executive Summary	10
1 Background of the document	11
1.1 Scope and Objectives	11
1.2 Content of the document	11
1.3 Related documents	11
1.3.1 Applicable documents	11
1.3.2 Input.....	11
1.3.3 Output.....	12
1.3.4 External documents	12
2 Review of Users Requirements	13
3 Methodology Description	16
3.1 Overview	16
3.2 Input data	17
3.2.1 SPOT/VEGETATION Collection 2 data	17
3.2.2 PROBA-V Collection 1 data	18
3.3 Output product	19
3.4 The retrieval Algorithm	20
3.4.1 Outline	20
3.4.2 Basic underlying assumptions.....	22
3.4.3 Related and previous applications.....	22
3.4.4 Alternative methodologies currently in use	23
3.4.5 Methodology.....	23
3.4.6 Quality Information	29
3.5 Limitations	31
3.6 Risk of failure and Mitigation measures	31
4 References	32
Annex 1: Coefficients for albedo calculation	35
Annex 2: Narrow-to-broadband conversion coefficients	36

List of Figures

Figure 1: Spectral Response Functions of VGT1, VGT2, and the three PROBA-V cameras, superimposed with a spectrum of green grass (Blue, Red, NIR and SWIR bands, respectively).	18
Figure 2: PROBA-V instrument layout.....	19
Figure 3: General physical concept of the albedo.....	20
Figure 4: Flow chart of the surface albedo algorithm, in relation to TOC-r retrieval	22
Figure 5: Illumination zenith angle dependence of the directional-hemispherical kernel integrals for the Roujean et al. (1992) model.	28

List of Tables

Table 1: GCOS Requirements for surface albedo as Essential Climate Variables.....	14
Table 2: WMO Requirements for Earth surface albedo [source: https://www.wmo-sat.info/oscar/variables/view/54].	15
Table 3: Spectral characteristics of VEGETATION 2 sensor	17
Table 4: Spectral characteristics of the PROBA-V sensor	19
Table 5 : Algorithm differences between successive versions of SA product.....	23
Table 6: Quality flag associated with the Surface Albedo	30
Table 7: Look-up table of directional-hemispherical and bi-hemispherical kernel integrals as a function of solar zenith angle for the Roujean et al. (1992) model.	35
Table 8: Narrow to broadband conversion coefficients for the SPOT/VEGETATION-2 channels. .	36
Table 9: Narrow to broadband conversion coefficients for the PROBA-V channels.	36

List of Acronyms

ALBH	Hemispherical Surface Albedo
ALDH	Directional Surface Albedo
ASTER	Advanced Spaceborne Thermal Emission and Reflection Radiometer
ATBD	Algorithm Theoretical Basis Document
AVHRR	Advanced Very High Resolution Radiometer
BOREAS	Boreal Ecosystem Atmosphere Study
BRDF	Bi-directional Reflectance Distribution Function
CEOS	Centre for Earth Observation Science
CGLS	Copernicus Global Land Service
CYCLOPES	Carbon cYcle and Change in Land Observational Products from an Ensemble of Satellites
ECV	Essential Climate Variable
FP-5, -6, -7	5 th , 6 th , 7 th Framework research Program of the European Union
GCOS	Global Climate Observing System
GLC2000	Global Land Cover map 2000
HAPEX-SAHEL	Hydrologic and Atmospheric Pilot Experiment in Sahel
LOPEX	Leaf Optical Properties Experiment
LSA-SAF	Land Surface Analysis – Satellite Applications Facility
METOP	Meteorological Operational
MISR	Multiangl e Imaging Spectro-Radiometer
MODIS	MODerate Imaging Spectrometer
NDVI	Normalised Difference Vegetation Index
NIR	Near InfraRed
NOAA	National Oceanic and Atmospheric Administration
NRT	Near Real Time
NWP	Numerical Weather Prediction
PAR	Photosynthetically Active Radiation
POLDER	Polarization and Directionality of the Earth's Reflectances, an instrument conceived by CNES to study clouds and aerosols
PROBA-V	The follow-on of SPOT5 / VEGETATION
PUM	Product User Manual
SA	Surface Albedo
SAIL	Scattering from Arbitrary Inclined Leaves
SEVIRI	Spinning Enhanced Visible and InfraRed Imager
SPOT	Satellite Probatoire d'Observation de la Terre

SWIR	Short-Wave InfraRed
TOA	Top Of Atmosphere
TOC	Top Of Canopy
TOC-r	Normalized Top Of Canopy Reflectance
TOPC	Terrestrial Observation Panel for Climate
USGS	United States Geological Survey
VGT	VEGETATION sensor onboard SPOT4 and SPOT5
VGT-P	Orbit segment (P) from VEGETATION sensor
VIS	VISible
VITO	Vlaamse Instelling voor Technologisch Onderzoek (Flemish Institute for Technological Research), Belgium
VNIR	Visible and Near Infrared
VSRF	Very Short-Range Forecasting
WMO	World Meteorological Organization

EXECUTIVE SUMMARY

The Copernicus Global Land Service (CGLS) is earmarked as a component of the Land service to operate “a multi-purpose service component” that provides a series of bio-geophysical products on the status and evolution of land surface at global scale. Production and delivery of the parameters take place in a timely manner and are complemented by the constitution of long-term time series.

The Surface Albedo retrieval algorithm was originally developed in the context of the FP5/CYCLOPES project for an application to SPOT/VEGETATION data. It has been then modified in the context of the FP6/VGT4Africa project for a near real time production. It was used to generate surface albedo products in the FP6/geoland project and its following FP7/geoland2 project, which provided a historical archive (1999-2012), derived from SPOT/VEGETATION Collection 2 sensor data. This historical archive was ingested in and the algorithm was originally used within the Copernicus Global Land service to generate the near real time (NRT) Surface Albedo products (2013-2014), derived from the SPOT/VEGETATION Collection 2 sensor data.

The algorithm was thereafter revised to continue the generation of NRT Surface Albedo products, derived from the PROBA-V Collection 1 sensor data (2014-NRT) at 1km spatial resolution.

This document presents the different algorithmic steps to retrieve the various albedo variables which make the Surface Albedo product of the Copernicus Global Land service.

1 BACKGROUND OF THE DOCUMENT

1.1 SCOPE AND OBJECTIVES

The objective of this document is to provide a detailed description and justification of the Version 1 of the retrieval algorithm of Surface Albedo (SA) Collection 1km.

The first issue of this document was to describe the necessary theoretical basis that underpins the implementation of the Copernicus Global Land SA product, derived from SPOT/VEGETATION. This updated version of the document (I2.10) reflects the adaptations of the algorithm applied on the PROBA-V Collection 1 input data.

1.2 CONTENT OF THE DOCUMENT

This document is structured as follows:

- Chapter 2 recalls the users requirements, and the expected performance
- Chapter 3 describes the retrieval methodology
- Chapter 4 lists the references

The parameters of the algorithm are given in the Annexes.

1.3 RELATED DOCUMENTS

1.3.1 Applicable documents

AD1: Annex I – Technical Specifications JRC/IPR/2015/H.5/0026/OC to Contract Notice 2015/S 151-277962 of 7th August 2015

AD2: Appendix 1 – Copernicus Global land Component Product and Service Detailed Technical requirements to Technical Annex to Contract Notice 2015/S 151-277962 of 7th August 2015

AD3: GIO Copernicus Global Land – Technical User Group – Service Specification and Product Requirements Proposal – SPB-GIO-3017-TUG-SS-004 – Issue I1.0 – 26 May 2015.

1.3.2 Input

Document ID	Descriptor
CGLOPS1_SSD	Service Specifications of the Global Component of the Copernicus Land Service.
CGLOPS1_ATBD_TOCR1km-V1.5	Algorithm Theoretical Basis Document of the normalized Top of Canopy Reflectance (TOC-r)

Collection 1Km Version 1.

1.3.3 Output

Document ID	Descriptor
CGLOPS1_PUM_SA1km-V1	Product User Manual describing all information about the SPOT/VGT & PROBA-V surface albedo Collection 1km Version 1 product
GIOGL1_VR_SA1km-V1	Validation Report of the SPOT/VGT surface albedo Collection 1km Version 1.4 products
CGLOPS1_VR_SA1km-PROBAV-V1.5	Validation Report of the PROBA-V surface albedo Collection 1km Version 1.5 products

1.3.4 External documents

MCD53_ATBD	MODIS BRDF/Albedo Product: algorithm theoretical basis document, version 5.0 (see https://modis-land.gsfc.nasa.gov/pdf/atbd_mod09.pdf)
PUM_PROBA-V-C1	Product User Manual PROBA-V Collection 1 (see http://www.vito-eodata.be/PDF/image/PROBAV-Products_User_Manual.pdf)

2 REVIEW OF USERS REQUIREMENTS

According to the applicable document [AD2] and [AD3], the user's requirements relevant for the surface albedo product are:

- **Definition:**
 - Refers to the hemispherically integrated reflectance of the Earth's surface in the range 0.4 – 0.7 μ m (or other specific short-wave) (CEOS)
 - Albedo is further defined spectrally (broadband) or for spectral bands of finite width, and according to its bi-directional reflectance properties (black-sky or white-sky albedo) (CEOS)

- **Geometric properties:**
 - Pixel size of output data shall be defined on a per-product basis so as to facilitate the multi-parameter analysis and exploitation.
 - The baseline datasets pixel size shall be provided, depending on the final product, at resolutions of 100m and/or 300m and/or 1km.
 - The target baseline location accuracy shall be 1/3rd of the at-nadir instantaneous field of view
 - pixel co-coordinates shall be given for centre of pixel

- **Geographical coverage:**
 - Geographic projection: regular lat-long
 - Geodetical datum: WGS84
 - Coordinate position: centre of pixel
 - Window coordinates:
 - Upper Left: 180°W-74°N
 - Bottom Right: 180°E 56°S

- **Ancillary information:**
 - the number of measurements per pixel used to generate the synthesis product
 - the per-pixel date of the individual measurements or the start-end dates of the period actually covered
 - quality indicators, with explicit per-pixel identification of the cause of anomalous parameter result

- **Accuracy requirements:**
 - **Baseline:** wherever applicable the bio-geophysical parameters should meet the internationally agreed accuracy standards laid down in document "Systematic Observation Requirements for Satellite-Based Products for Climate". Supplemental details to the satellite based component of the "Implementation Plan for the Global

- Observing System for Climate in Support of the UNFCCC (GCOS-154, 2011)" (Table 1)
- **Target:** considering data usage by that part of the user community focused on operational monitoring at (sub-) national scale, accuracy standards may apply not on averages at global scale, but at a finer geographic resolution and in any event at least at biome level.

Table 1: GCOS Requirements for surface albedo as Essential Climate Variables.

Variable/ Parameter	Horizontal Resolution	Temporal Resolution	Accuracy	Stability
Black and White-sky albedo (GCOS#154, 2011)	1 km	Daily to weekly	Max(5%; 0.0025)	Max(1%; 0.0001)
Black and White-sky albedo (GCOS#200, 2016)	200/500m	Daily	Max(5%; 0.0025)	Max(1%; 0.001)

In a recent update of the GCOS requirements [GCOS#200, 2016], there is a distinction between the products targeted for “adaptation” and “modeling” that results in different needs for the horizontal resolution. In CGLS, we focus on modeling requirements as they are the main users targeted (Table 1). Note, as well, that the figure for stability requirements in absolute term has been corrected (0.001 instead of 0.0001)

Other requirements come from the “WMO Rolling Requirement Review” that aids the setting of the priorities to be agreed by WMO Members and their space agencies for enhancing the space based Global Observing System. In this context, GCOS has provided input for the systematic climate observation elements of the “WMO Observing Requirements Database” (<https://www.wmo-sat.info/oscar/variables/view/54>). The GCOS requirements are only partly consistent with this process in that they provide only target but not “breakthrough” or “threshold” (i.e. minimum) requirements. GCOS also provides requirements on stability that are not currently included in the WMO requirements database.

The “WMO Observing Requirements Database” specifies requirements on the surface albedo for climatologic applications at three quality levels (Table 2):

- Threshold (T): Minimum requirement;
- Breakthrough (B): Significant improvement;
- Goal (G): Optimum, no further improvement required

The WMO Observing Requirements Database specifies uncertainties in absolute parameter units. The stated “goal” uncertainty requirement of 5% is thus equivalent to ± 0.05 .

Table 2: WMO Requirements for Earth surface albedo [source: <https://www.wmo-sat.info/oscar/variables/view/54>].

Application	Uncertainty (%)			Horizontal resolution (km)			Observing cycle (h:hours, d:days)			Timeliness (h:hours, d:days)		
	G	B	T	G	B	T	G	B	T	G	B	T
High resolution NWP	5	10	20	0.5	4	10	1h	3h	12h	1h	3h	12h
Nowcasting/VSRF	5	10	20	1	5	10	1d	3d	10d	0.5d	1d	3d
Climate-TOPC (deprecated)	5	7	10	1	2	10	1d	3d	30d	30d	45d	90d

3 METHODOLOGY DESCRIPTION

3.1 OVERVIEW

GCOS established a list of Essential Climate Variables (ECV) that characterize the state of the global climate system and its evolution resulting from natural and anthropogenic forcing (GCOS, 2003, 2006). Among them, one key terrestrial variable is the surface albedo, which is both a forcing variable controlling the surface energy budget and a sensitive indicator of environmental changes including land degradation.

If the long time series of NOAA/AVHRR instrument first made possible to study the land surface properties at global scale, more recent instruments capable of performing multi-angular measurements such as POLDER, MODIS, MISR, SEVIRI are particularly well-suited for characterizing the directional reflectance properties and, hence, for estimating the albedo. Then, the availability of operational surface albedo products since year 2000 constitutes a significant achievement for the science community (e.g., Schaaf et al., 2002; Martonchik et al., 1998), especially for applications concerning the analysis and simulation of the Earth climate and its variability.

A robust method for albedo determination from remote sensing data consists in separating the different elements of the processing chain: atmospheric correction, directional reflectance normalisation, spectral albedo calculation, and, finally, the narrow-to-broadband albedo conversion. Such an approach was adopted for retrieving the albedo products in near-real time derived from POLDER (Leroy et al., 1997), MODIS (Strahler et al., 1999), and SEVIRI (Geiger et al., 2008, Carrer et al., 2010) in the framework of the LSA-SAF.

A more rigorous approach from a theoretical point of view is to treat the radiative transfer problem in the coupled surface-atmosphere system simultaneously. This is achieved in the algorithms implemented for the derivation of surface albedo from the MISR instrument (Diner et al., 1999) and from Meteosat (Pinty et al., 2000, Govaerts et al., 2008). Liang (2003) discussed a method relating the observed Top-of-the-Atmosphere (TOA) reflectances directly to broadband surface albedo.

The former approach was chosen to develop the first albedo retrieval algorithm using SPOT/VEGETATION sensor data like input in the FP5/CYCLOPES project. Indeed, it is a good compromise between quality of the results, easiness of implementation, and computation time. This explains why it is used in operational context (MODIS program, LSA-SAF). After an adaptation to a near-real-time application in the frame of the FP6 VGT4Africa project, the methodology was applied over the existing SPOT/VEGETATION Collection 2 time series in the FP7/geoland2 project. Since 1st January 2013, the SPOT/VEGETATION surface albedo is generated in the Copernicus Global Land service (<http://land.copernicus.eu/global>). Due to the discontinuation of the SPOT/VEGETATION mission in May 2014, the surface albedo is derived from the PROBA-V Collection 1 dataset.

3.2 INPUT DATA

The input data of the Surface Albedo processing line are the spectral directional parameters resulting from the BRDF model inversion on the TOC reflectances [CGLOPS1_ATBD_TOCR1km-V1.5]. The TOC reflectances are derived from the standard VGT-P TOA reflectances provided by the SPOT/VEGETATION ground segment and from the standard L2A TOA reflectances provided by the PROBA-V ground segment.

3.2.1 SPOT/VEGETATION Collection 2 data

The SPOT/VEGETATION Collection 2 (C2) input data are the standard VGT-P 1km (Top of Atmosphere - daily orbit reflectance) products generated and provided by the SPOT VEGETATION programme through the VITO ground segment (<http://free.vgt.vito.be/>).

From April 1998 to May 2014, the VEGETATION sensor was operational on board the SPOT 4 and 5 Earth observation satellite systems, providing a global observation of the world on a daily basis. The instrumental concept relies on a linear array of 1728 CCD detectors with a large field of view (101°) in four optical spectral bands described in Table 3 and Figure 1. At the radiometric level, the two VEGETATION instruments are very similar, but yet there are some differences. Firstly, the spectral bands of the VGT1 and VGT2 sensors have been defined as alike as possible, but the spectral response functions are not identical (Figure 1) (Fensholt et al. 2009) causing small differences in radiometric response. The VGT website reports changes up to 1.6% for Blue, 5.4% for Red, 2.5% for NIR, 4.6% for SWIR and 12.1% for NDVI for vegetated surfaces (<http://www.vgt.vito.be/faqnew/>). Secondly, there is a difference in calibration accuracy due to the improved calibration methods used for VGT2. The effect is small for most spectral bands, but can result in a reflectance bias of 6.3% for NIR (<http://www.vgt.vito.be/faqnew/>).

Table 3: Spectral characteristics of VEGETATION 2 sensor

Acronym	Centre (nm)	Width (nm)	Potential Applications
B0	450	40	Continental ecosystems - Atmosphere
B2	645	70	Continental ecosystems
B3	835	110	Continental ecosystems
SWIR	1665	170	Continental ecosystems

The spatial resolution is 1.15 km at nadir and presents minimum variations for off-nadir observations. The 2200 km swath width implies a maximum off nadir observation angle of 50.5°. About 90% of the equatorial areas are imaged each day, the remaining 10% being imaged the next day. For latitudes higher than 35° (North and South), all regions are acquired at least once a day. The multi-temporal registration is about 300 meters.

3.2.2 PROBA-V Collection 1 data

The PROBA-V input data are the standard Collection 1 (C1) L2A 1km (Top of Atmosphere -daily orbit reflectance) products generated and provided by the PROBA-V ground segment through VITO (<http://proba-v.vgt.vito.be/>).

The PROBA-V satellite was launched at 6th May 2013 and was designed to bridge the gap in space-borne vegetation measurements between SPOT-VGT (March 1998 – May 2014) and the Sentinel-3 satellites launched in 2016. The mission objective is to ensure continuity with the heritage of the SPOT-VGT mission.

PROBA-V operates at an altitude of 820 km in a sun-synchronous orbit with a local overpass time at launch of 10:45 h. Because the satellite has no onboard propellant, the overpass time is expected to gradually differ from the at-launch value. The instrument has a Field Of View of 102°, resulting in a swath width of 2295 km. This swath width ensures a daily near-global coverage (90%) and full global coverage is achieved every 2 days.

The optical design of PROBA-V consists of three cameras. Each camera has two focal planes, one for the short wave infrared (SWIR) and one for the visible and near-infrared (VNIR) bands. The VNIR detector consists of four lines of 5200 pixels. Three spectral bands were implemented, comparable with SPOT-VGT: BLUE, RED, and NIR (see Table 4). The SWIR detector contains the SWIR spectral band and is a linear array composed of three staggered detectors of 1024 pixels. The spectral response functions of the four spectral bands from the three PROBA-V cameras are compared to those of SPOT/VEGETATION-1 and -2 in Figure 1.

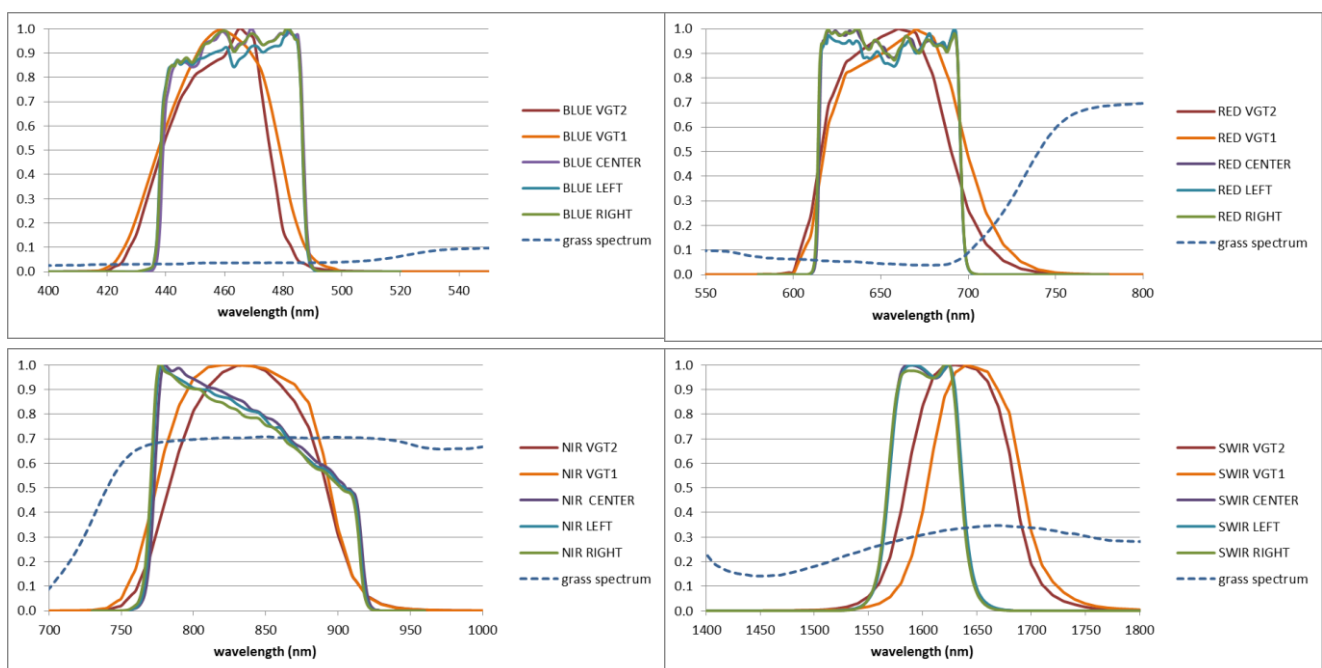


Figure 1: Spectral Response Functions of VGT1, VGT2, and the three PROBA-V cameras, superimposed with a spectrum of green grass (Blue, Red, NIR and SWIR bands, respectively).

Table 4: Spectral characteristics of the PROBA-V sensor

Acronym	Centre (nm)	Width (nm)	Potential Applications
B0	463	46	Continental ecosystems - Atmosphere
B2	655	79	Continental ecosystems
B3	845	144	Continental ecosystems
SWIR	1600	73	Continental ecosystems

The instrument plane layout is shown in Figure 2. Observations are taken at resolutions between 100 m and 180 m at nadir up to 350 m and 660 m at the swath extremes for the VNIR and SWIR channels, respectively (Francois et al. 2014). Final PROBA-V products are disseminated at 333 m and 1 km resolution.

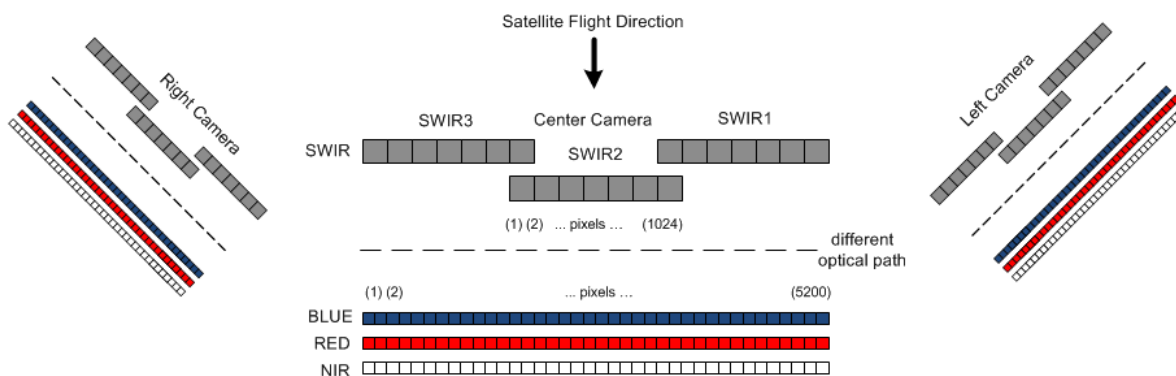


Figure 2: PROBA-V instrument layout

More information on the PROBA-V processing can be found in Sterckx et al. (2014) and Dierckx et al. (2014). Information on the PROBA-V Collection 1 is available on <http://proba-v.vgt.vito.be/content/collection-1-change-summary>.

3.3 OUTPUT PRODUCT

The CGLS Surface Albedo products are made of 2 products defined as follows:

1. Directional Albedo (ALDH), at local solar noon, which contains:
 - a. The broadband Directional Hemispheric reflectance over visible band [0.4, 0.7 μ m], and its error
 - b. The broadband Directional Hemispheric reflectance over near infrared band [0.7-4 μ m], and its error

- c. The broadband Directional Hemispheric Reflectance over total spectrum [0.3-4 μ m], and its error
2. Hemispheric Albedo (ALBH) which contains:
 - a. The broadband Bi-Hemispheric Reflectances over visible band [0.4, 0.7 μ m], and its error
 - b. The broadband Bi-Hemispheric Reflectances over near-infrared band [0.7-4 μ m], and its error
 - c. The broadband Bi-hemispheric Reflectances over total spectrum [0.3-4 μ m], and its error

Both products contains also:

- The quality flag of the product
- The number of valid observations used for the BRDF model inversion (NMOD)
- A land-sea mask based upon the GLC-2000 land cover map (Bartholomé et Belward, 2005)

Note that the spectral albedos are not disseminated.

The detailed description of the output products are given in the Product User Manual [CGLOPS1_PUM_SA1km-V1].

3.4 THE RETRIEVAL ALGORITHM

3.4.1 Outline

The surface albedo quantifies the fraction of the irradiance reflected by the surface of the Earth. It provides information on the radiative balance, thus on the temperature and water balance. It can be measured taking into account the general physical concept described below (Figure 3).

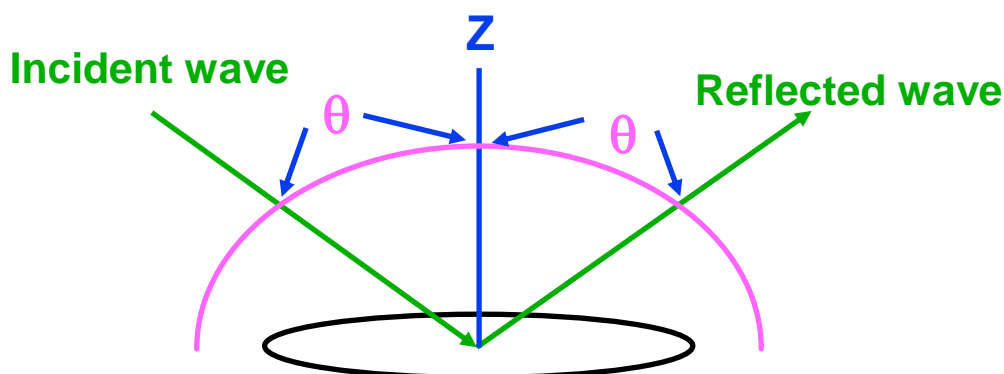


Figure 3: General physical concept of the albedo

The directional albedo (a^{dh}) or directional-hemispherical reflectance (also called black-sky albedo) is defined as the integration of the bi-directional reflectance over the viewing hemisphere. It assumes all energy is coming from a direct radiation from the sun. It is computed for the local solar noon.

$$a^{dh}(\lambda, \theta_s, \varphi_s) = \frac{1}{\pi} \int_0^{2\pi} \int_0^{\pi/2} \rho_\lambda(\theta_s, \theta_v, \varphi) \cdot \cos\theta_v \cdot \sin\theta_v \cdot d\theta_v \cdot d\varphi \quad \text{Eq. 1}$$

The hemispherical albedo (a^{bh}) or bi-hemispherical reflectance (also called white-sky albedo) is defined as the integration of the directional albedo over the illumination hemisphere. It assumes a complete diffuse illumination. It is computed as:

$$a^{bh}(\lambda) = \frac{1}{\pi} \int_0^{2\pi} \int_0^{\pi/2} a^{dh}(\lambda, \theta_s, \varphi_s) \cos\theta_s \sin\theta_s d\theta_s d\varphi_s \quad \text{Eq. 2}$$

The spectrally-integrated albedos are called broadband albedos as:

$$a = \frac{\int_{300\text{nm}}^{4000\text{nm}} E(\lambda) \cdot a(\lambda) d\lambda}{\int_{300\text{nm}}^{4000\text{nm}} E(\lambda) d\lambda} \quad \text{Eq.3}$$

Three broadband albedos are defined:

- Over the visible (PAR) range [0,4µm – 0,7µm]
- Over the near-infrared range [0,7µm – 4µm]
- Over the total shortwave band [0,3µm – 4µm] (Eq.3)

The retrieval algorithm follows the approach separating atmospheric correction, directional reflectance normalization, and albedo determination (Figure 4). The processing steps starting from TOA reflectances to obtain the BRDF parameters are common with the normalized Top of Canopy (TOC) reflectances chain. They are described in details in the TOC-r ATBD [CGLOPS1_ATBD_TOCR1km-V1.5].

Here, only the angular integration and the spectral integration which allow calculating the albedo variables from the Bidirectional Reflectance Distribution Function (BRDF) parameters are presented.

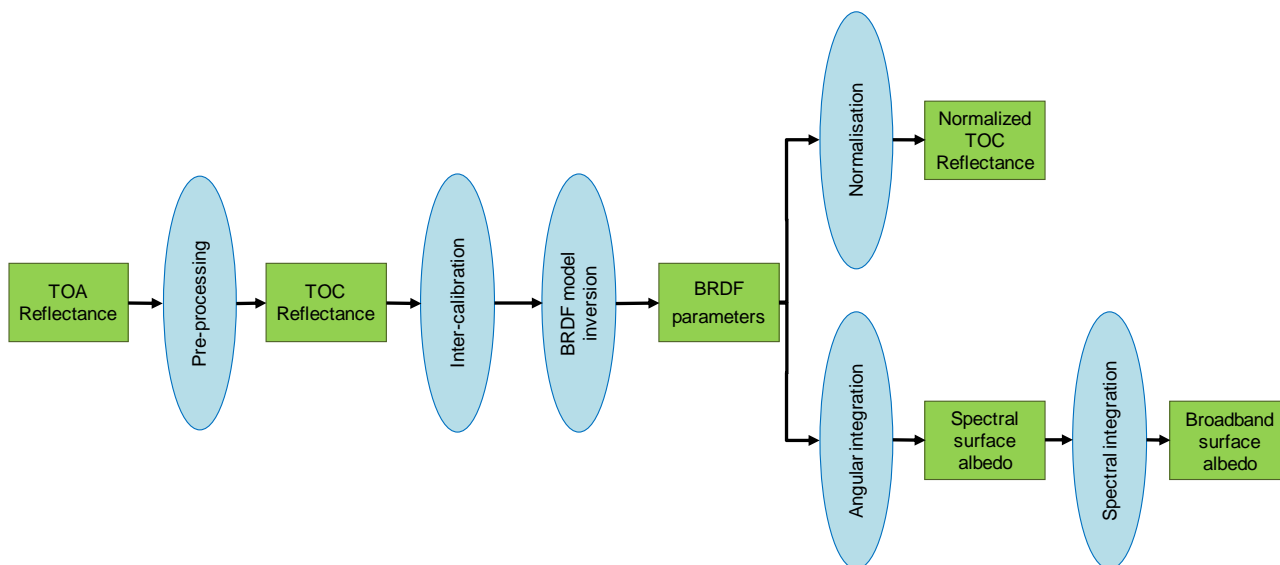


Figure 4: Flow chart of the surface albedo algorithm, in relation to TOC-r retrieval

3.4.2 Basic underlying assumptions

The objective for disseminating both visible and near infrared surface albedo products is that it is found useful to complete the surface energy budget. Note incidentally that the spectral range of visible chosen here corresponds to the PAR (Photosynthetically Active Radiation) domain and therefore could be used to conduct studies on carbon budget. Vegetation absorbs most of the visible radiation, and the phenomenon is very sensitive to the greenness. On the other hand, at the exception of woody material, leafy vegetation will reflect most of near infrared radiation. For sparse canopies showing a large proportion of soil background, the problem can be more complex. The impact on the short-wave (solar) albedo can be tenuous because of the counter-balancing between broadband visible and near infrared surface albedo. This fully justifies the dissemination of the three broadband albedos although one could be derived from the two others.

3.4.3 Related and previous applications

The differences in algorithms between the surface albedo V1.5 product and its previous versions are summarized in Table 5. The product remains updated every 10 days, with a temporal basis for compositing of 30 days and delivered with 12 days lag in Near Real Time (NRT).

In V1.4 or earlier versions, a snow detection mechanism was implemented based on spectral variations of snow (Dozier, 1989) as a set of thresholds on TOA reflectances and the Normalized Difference Snow Index (NDSI). This approach is not used in the current version (V1.5 or later) anymore and replaced by directly using the PROBA-V Collection 1 [PUM_PROBA-V-C1] Status Maps to identify snow/ice.

Similarly, in V1.4 or earlier versions, a cloud detection mechanism was implemented based on the same screening method developed by Hagolle et al. (2004), with thresholds associated to each of the bands empirically tuned and validated at global scale in April 1999. This latter approach is not used in the current version (V1.5 or later) anymore and replaced by directly using the PROBA-V Collection 1 [PUM_PROBA-V-C1] Status Maps to identify clouds.

Table 5 : Algorithm differences between successive versions of SA product

Surface albedo versions	Algorithm differences
Version 1.4 or earlier	SPOT/VGT Collection 2 input data. Own snow & cloud detection. Inter-calibration to POLDER sensor.
Version 1.5 or later	PROBA-V Collection 1 input data (2014-NRT). Snow & cloud detection based on Status Map of input data. Inter-calibration to SPOT/VGT2.

3.4.4 Alternative methodologies currently in use

The Bidirectional Reflectance Distribution Function (BRDF)/Albedo products (MCD43) from MODIS Land are calculated with models that describe the differences in radiation due to the scattering (anisotropy) of each pixel, relying on multi-date, atmospherically corrected, cloud-cleared input data measured over 16-day period integrating both TERRA/MODIS and AQUA/MODIS input data [MCD53_ATBD].

3.4.5 Methodology

As shown in Figure 4, the surface albedo algorithm relies on the TOC-r [CGLOPS1_ATBD_TOCR1km-V1.5] algorithm and hence uses the BRDF parameters written during the TOC-r processing as input. The algorithm detailed below presents the calculation of the integrals of Eq.7 and Eq.8 for determining the albedo estimates a_j^{dh} and a_j^{bh} in all sensor channels by applying the coefficients k_j provided by the directional normalization. The narrow band albedo values are considered as an approximation to the spectral albedo at the central wavelength λ_j of the channel. Furthermore, broadband albedo values a_γ^{dh} and a_γ^{bh} corresponding to suitable ranges $\gamma = [\lambda_1, \lambda_2]$ are derived from the spectral estimates by using appropriate approximations to the integrals of Eq.12 and of Eq.13.

3.4.5.1 Physical background

The spectral albedo of a plane surface is defined as the ratio between the hemispherical integrals of the up-welling (reflected) spectral radiance $L^\uparrow(\lambda, \theta_{out}, \phi_{out})$ and the down-welling spectral radiance $L^\downarrow(\lambda, \theta_{in}, \phi_{in})$ weighted by the cosine of the angle between the respective reference direction and the surface normal:

$$a(\lambda) = \frac{\int L^\uparrow(\lambda, \theta_{out}, \phi_{out}) \cos \theta_{out} d\Omega_{out}}{\int_{2\pi} L^\downarrow(\lambda, \theta_{in}, \phi_{in}) \cos \theta_{in} d\Omega_{in}} \quad \text{Eq. 4}$$

Where $d\Omega_{out} = \sin \theta_{out} d\theta_{out} d\phi_{out}$ and $d\Omega_{in} = \sin \theta_{in} d\theta_{in} d\phi_{in}$. The expression in the denominator defines the spectral irradiance $E^\downarrow(\lambda)$. By introducing the bi-directional reflectance factor R, the up-welling radiance distribution can be expressed in terms of the down-welling radiation as

$$L^\uparrow(\lambda, \theta_{out}, \phi_{out}) = \frac{1}{\pi} \int_{2\pi} R(\lambda, \theta_{out}, \phi_{out}, \theta_{in}, \phi_{in}) L^\downarrow(\lambda, \theta_{in}, \phi_{in}) \cos \theta_{in} d\Omega_{in} \quad \text{Eq.5}$$

And Eq.4 becomes

$$a(\lambda) = \frac{\frac{1}{\pi} \int_{2\pi} \int_{2\pi} R(\lambda, \theta_{out}, \phi_{out}, \theta_{in}, \phi_{in}) L^\downarrow(\lambda, \theta_{in}, \phi_{in}) \cos \theta_{in} \cos \theta_{out} d\Omega_{in} d\Omega_{out}}{E^\downarrow(\lambda)} \quad \text{Eq.6}$$

From the result, it can be seen that, in general, the spectral albedo of non-Lambertian surfaces depends on the angular distribution of the incident radiation, which in turn depends on the concentration and properties of scattering elements (e.g. aerosols) in the atmosphere and, on particular, on the presence of clouds. Therefore, the spectral albedo is not a true surface property but rather a characteristic of the coupled surface-atmosphere system.

In the idealized case of purely direct illumination at incidence angles (θ_{dh}, ϕ_{dh}) , the down-welling radiance is given by $L^\downarrow(\lambda, \theta_{in}, \phi_{in}) = \sin^{-1} \theta_{dh} \delta(\theta_{in} - \theta_{dh}, \phi_{in} - \phi_{dh}) E_0(\lambda)$, which results in

$$E^\downarrow(\lambda) = E_0(\lambda) \cos \theta_{dh} \quad \text{and} \quad L^\uparrow(\lambda, \theta_{out}, \phi_{out}, \theta_{dh}, \phi_{dh}) = \frac{1}{\pi} R(\lambda, \theta_{out}, \phi_{out}, \theta_{dh}, \phi_{dh}) E_0(\lambda) \cos \theta_{dh}. \quad \text{By}$$

inserting these expressions into Eq.4 and Eq.6, we obtain the spectral directional-hemispherical (or “black-sky”) albedo $a^{dh}(\lambda, \theta_{dh}, \phi_{dh})$:

$$a^{dh}(\lambda, \theta_{dh}, \phi_{dh}) = \frac{1}{\pi} \int_{2\pi} R(\lambda, \theta_{out}, \phi_{out}, \theta_{dh}, \phi_{dh}) \cos \theta_{out} d\Omega_{out} \quad \text{Eq.7}$$

On the other hand, for completely diffuse illumination the down-welling radiance $L^\downarrow(\lambda, \theta_{in}, \phi_{in}) = L_0(\lambda)$ is constant and the irradiance becomes $E^\downarrow(\lambda) = \pi L_0(\lambda)$. By inserting these terms into Eq.6 and after making use of Eq.7, the spectral bi-hemispherical (or “white-sky”) albedo $a^{bh}(\lambda)$ can be written as:

$$a^{bh}(\lambda) = \frac{1}{\pi} \int_{2\pi} a^{dh}(\lambda, \theta_{in}, \phi_{in}) \cos \theta_{in} d\Omega_{in} \quad \text{Eq.8}$$

These two quantities are true surface properties and correspond to the limiting cases of point source $[a^{dh}(\lambda, \theta_{dh}, \phi_{dh})]$ and completely diffuse illumination $[a^{bh}(\lambda)]$. For partially diffuse illumination, the actually occurring spectral albedo value may be approximated as a linear combination of the limiting cases as follows:

$$a(\lambda) = [1 - f_{diffuse}(\lambda)] a^{dh}(\lambda, \theta_s, \phi_s) + f_{diffuse}(\lambda) a^{bh}(\lambda) \quad \text{Eq.9}$$

Where $f_{diffuse}$ denotes the fraction of diffuse radiation and (θ_s, ϕ_s) the solar direction.

For some users, the quantity of interest is not the spectral but rather the broadband albedo, which is defined as the ratio of up-welling to down-welling radiation fluxes in a given wavelength interval $[\lambda_1, \lambda_2]$:

$$a_{[\lambda_1, \lambda_2]} = \frac{F_{[\lambda_1, \lambda_2]}^\uparrow}{F_{[\lambda_1, \lambda_2]}^\downarrow} = \frac{\int_{\lambda_1}^{\lambda_2} \int_{2\pi} L^\uparrow(\lambda, \theta_{out}, \phi_{out}) \cos \theta_{out} d\Omega_{out} d\lambda}{\int_{\lambda_1}^{\lambda_2} \int_{2\pi} L^\downarrow(\lambda, \theta_{in}, \phi_{in}) \cos \theta_{in} d\Omega_{in} d\lambda} \quad \text{Eq.10}$$

In analogy to Eq.6, it can be expressed in terms of the bi-directional reflectance factor as:

$$a(\lambda) = \frac{\frac{1}{\pi} \int_{\lambda_1}^{\lambda_2} \int_{2\pi} \int_{2\pi} R(\lambda, \theta_{out}, \phi_{out}, \theta_{in}, \phi_{in}) L^\downarrow(\lambda, \theta_{in}, \phi_{in}) \cos \theta_{in} \cos \theta_{out} d\Omega_{in} d\Omega_{out} d\lambda}{F_{[\lambda_1, \lambda_2]}^\downarrow} \quad \text{Eq.11}$$

The directional-hemispherical broadband albedo

$$a_{[\lambda_1, \lambda_2]}^{dh}(\theta_{dh}, \phi_{bh}) = \frac{\int_{\lambda_1}^{\lambda_2} a^{dh}(\lambda, \theta_{dh}, \phi_{bh}) E^\downarrow(\lambda) d\lambda}{\int_{\lambda_1}^{\lambda_2} E^\downarrow(\lambda) d\lambda} \quad \text{Eq.12}$$

and the bi-hemispherical broadband albedo

$$a_{[\lambda_1, \lambda_2]}^{bh} = \frac{\int_{\lambda_1}^{\lambda_2} a^{bh}(\lambda) E^\downarrow(\lambda) d\lambda}{\int_{\lambda_1}^{\lambda_2} E^\downarrow(\lambda) d\lambda} \quad \text{Eq.13}$$

can be written as integrals of the respective spectral quantities weighted by the spectral irradiance. At the opposite of the spectral albedo defined in Eq.7 and Eq.8, the broadband albedo values are not pure surface properties since the wavelength dependence of the spectral irradiance $E(\lambda)$ appearing as a weight factor in their definition may vary as a function of the atmospheric composition. In analogy to Eq.9, the broadband albedo for partially diffuse illumination conditions may be expressed as a weighted average of $a_{[\lambda_1, \lambda_2]}^{dh}(\theta_s, \phi_s)$ and $a_{[\lambda_1, \lambda_2]}^{bh}$.

3.4.5.2 Angular integration

In the “BRDF model inversion step” (Figure 4), the semi-empirical kernel-based reflectance model of Roujean et al. (1992) is adjusted to the TOC reflectances. This yields an estimate of the total angular dependence of the bi-directional reflectance factor R_j in the spectral channel j of the sensor:

$$R_j(\theta_{out}, \theta_{in}, \phi) = k_j * f(\theta_{out}, \theta_{in}, \phi) \quad \text{Eq. 14}$$

Here $k_j = (k_{0j}, k_{1j}, k_{2j}, \dots)^T$ and $f = (f_0, f_1, f_2, \dots)^T$ represent vectors formed by the retrieved model parameters k_{ij} and the kernel functions f_j , respectively. The individual azimuth angles were replaced by the relative azimuth angle ϕ between the directions of incoming and outgoing light paths. This is possible without restrictions of generality as long as the surface is considered as spatially isotropic.

Inserting the reflectance model in Eq. 14 in the Eq.7 and Eq.8 gives the expressions

$$a_j^{dh}(\theta_{in}) = \mathbf{k}_j * \mathbf{I}^{dh}(\theta_{in}) \quad \text{and} \quad a_j^{bh} = \mathbf{k}_j * \mathbf{I}^{bh} \quad \text{Eq.15}$$

for the spectral albedo quantities, where

$$I_i^{dh}(\theta_s) = \frac{1}{\pi} \int_0^{2\pi} \int_0^{\pi/2} f_i(\theta_{out}, \theta_{in}, \phi) \cos(\theta_{out}) \sin(\theta_{in}) d\theta_{out} d\phi$$

and

$$I_i^{bh} = 2 \int_0^{\pi/2} I_i^{dh}(\theta_{in}) \cos(\theta_{in}) \sin(\theta_{in}) d\theta_{in} \quad \text{Eq.16}$$

are the respective angular integral of the fixed kernel functions which can conveniently be pre-computed and stored in look-up tables. Figure 5 shows the illumination angle dependence of the directional-hemispherical integral of the three kernels of the Roujean et al. (1992) model. The Numerical values are listed in Annex 1: .

The directional-hemispherical integral $I_1^{dh}(\theta)$ of the geometric kernel diverges for the large illumination zenith angles. This may lead to a potential problem for the directional-hemispherical albedo when the reference angle is larger than 70° . However, under such conditions, the fraction of diffuse radiation is rather large and the directional-hemispherical albedo may then be of little relevance for practical purposes. The bi-hemispherical integral of f_1 remains finite owing to the weighting of the kernel with the cosine of the illumination angle. The numerical values of the bi-hemispherical integrals are also given in Annex 1: .

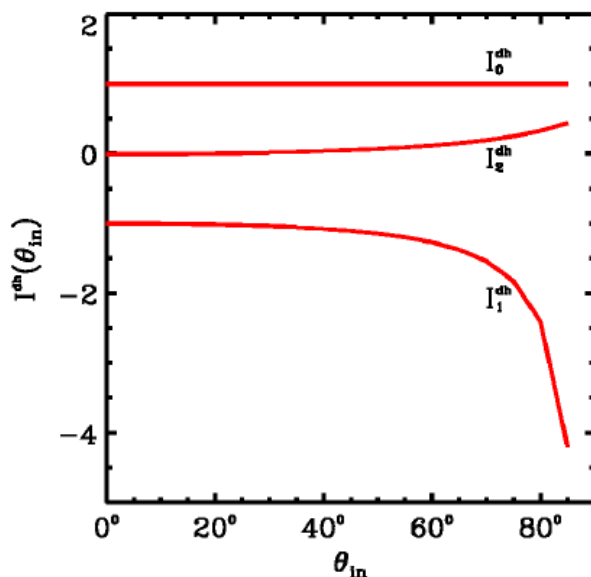


Figure 5: Illumination zenith angle dependence of the directional-hemispherical kernel integrals for the Roujean et al. (1992) model.

3.4.5.3 Spectral integration

The kernel approach offers a description of the angular dependence of the reflectance factor. It is applied to each channel of the sensor separately and provides no information on the spectral behavior outside the available bands. Broadband albedo is defined as the integral of spectral albedo over a certain wavelength interval weighted by the spectral irradiance (Eq.12 and Eq.13). Since the integral can be approximated as a weighted sum of the integrand at discrete values of the integration variable, broadband albedo may be expressed as a linear combination of the spectral albedo values in the available spectral bands.

Samain (2006) determined equations for the conversion from spectral albedo to various broadband albedo ranges. The SAIL radiative transfer model (Verhoef, 1984) was used to generate an extensive data set of synthetic spectral canopy reflectances for a wide range of soil and leaf optical properties. A data set comprising 11 representative soil and 108 vegetation types was constituted from the ASTER (Hook, 1998) and USGS spectral libraries, the LOPEX'93 experiment (Hosgood et al., 1995), and the BOREAS and HAPEX-SAHEL field campaigns. Simulations with the PROSPECT model (Jacquemoud and Baret, 1990) complete the dataset to represent senescent leaves. Similar studies were performed by Liang (2000) for various other satellite instruments.

The retrieved coefficients are applied both for the directional-hemispherical albedo and for the bi-hemispherical albedo.

A specific set of coefficients is given in the case where snow is detected, and also considering the cases when the B0 (blue) and B3 (near-infrared) bands are saturated. The coefficients, valid for the VEGETATION-2 sensor, and the coefficients for the PROBA-V sensor, are given in Table 8 and Table 9 in Annex 2: Narrow-to-broadband conversion coefficients.

3.4.5.4 Algorithm description

The albedo algorithm operates on a “pixel by pixel” basis. The variable reference angle θ_{dh} (local solar noon) for the directional-hemispherical albedo needs to be determined as a function of the pixel’s geographic coordinates and the day of the year. The corresponding directional-hemispherical kernel integrals $\hat{I}^{dh}(\theta_{dh})$ are linearly interpolated from a pre-calculated look-up table (Table 7 in Annex 1:). The spectral directional-hemispherical albedo can then be calculated for each spectral band j as a linear combination of the kernel integrals according to

$$a_j^{dh}(\theta_{dh}) = \mathbf{k}_j * \hat{\mathbf{I}}^{dh} \quad \text{Eq.17}$$

The spectral bi-hemispherical albedo values are determined as

$$a_j^{bh} = \mathbf{k}_j * \mathbf{I}^{bh} \quad \text{Eq.18}$$

with fixed values for the elements of \mathbf{I}^{bh} .

The broadband albedo values are derived from the spectral quantities by applying the linear transformation

$$a_\gamma^{xh} = c_{0\gamma}^{xh} + \sum_j c_{j\gamma}^{xh} a_j^{xh} \quad (\text{“x” = “d” or “b”}) \quad \text{Eq.19}$$

with coefficients $c_{0\gamma}^{xh}$ and $c_{j\gamma}^{xh}$ determined by the regression analysis described in 3.4.5.3.

Annex 2 contains sets of coefficients used to calculate the broadband directional-hemispherical as well as the broadband bi-hemispherical albedo quantities. In order to apply the above equation for broadband calculation, it is essential that spectral albedo estimates be available for all channels considered in the regression study. In order to better take into account the differences in the spectral properties of various surface conditions, sets of regression coefficients depend on the presence of snow.

3.4.6 Quality Information

Thanks to the linear relationship between the BRDF model parameters and the spectral albedo quantities, standard (“1-sigma”) error estimates for the latter can conveniently be retrieved from the error covariance matrix \mathbf{C}_k of the model parameters (Lutch and Lewis, 2000).

$$\sigma[a_j] = \sqrt{\mathbf{I}^T \mathbf{C}_k \mathbf{I}} \quad \text{Eq.20}$$

Assuming that the errors of the spectral albedo values are uncorrelated, the error estimate for broadband albedo quantities is given by

$$\sigma[a_\gamma^{xh}] = \sqrt{\sigma^2[\text{regression}] + \sum_j (c_{j\gamma}^{xh})^2 \sigma^2[a_j^{xh}]} \quad (\text{"x"} = \text{"d"} \text{ or } \text{"b"}) \quad \text{Eq.21}$$

where $\sigma^2[\text{regression}]$ denotes the residual variance of the linear regression.

These (theoretical) error estimates for the generated albedo parameters represent the most general quality indicator delivered by the algorithm. Since all transformations applied to derive albedo are linear, the validity of the Gaussian assumption for the error structure of the input data propagates to the retrieved albedo estimates. The validity of the theoretical error estimates is strictly speaking restricted to the framework of the applied BRDF-model.

Further, a quality flag is provided giving information about the different steps of the algorithm (Table 6).

Table 6: Quality flag associated with the Surface Albedo. "XX" on bits 7, 8 and 9 means "DH" or "BH" depending on the product.

* indicates propagated from TOC-r Quality flag	Bit = 0	Bit = 1
Bit 1*: Land/Sea	Land	Sea
Bit 2*: Snow status	Clear	Snow
Bit 3*: Cloud/Shadow status	Clear	Suspect
Bit 4*: Aerosol status	Pure	Mixed
Bit 5*: Aerosol source	MODIS	Latitudinal gradient
Bit 6*: Input Status	OK	Out of range or invalid
Bit 7: AL-XX-VI status	OK	Out of range or invalid
Bit 8: AL-XX-NI status	OK	Out of range or invalid
Bit 9: AL-XX-BB status	OK	Out of range or invalid
Bit 10*: Red band (B2) saturation status	OK	Saturated
Bit 11*: Blue band (B0) saturation status	OK	Saturated

3.5 LIMITATIONS

The main limitation of the Surface Albedo product is the length of the composition period. 30 days are necessary to guarantee a minimum of cloudless scenes at global scale. However, this yields obviously some limitations in regard to the capability of the SA product to capture the evolution of some targets with a sufficient degree of accuracy, especially during the period when the state of the surface changes rapidly.

Cloud pixels at the border of the orbit segment can result in an underestimate of cloud shadow (in case projected outside the segment), or cloud dilate (in case radius of spheric morphologic filter falls outside the segment) in the TOC-r pre-processing [CGLOPS1_ATBD_TOCR1km-V1.5]. In such case, shadow pixels are used as 'clear' and, hence, can introduce some noise in the BRDF model inversion.

Any misclassification of cloud and snow pixels in the input data can introduce some noise in the albedo products unless the additional rules in the TOC-r pre-processing [CGLOPS1_ATBD_TOCR1km-V1.5] overrule this classification. For instance, overestimating clouds reduce the number of valid observations for the BRDF model inversion. In the worst case, the inversion is not possible and the albedo value is missing; in better case, the BRDF model is less constraint during the inversion and the resulting uncertainty is higher on the retrieved albedo value. Another impact is that clouds wrongly identify as "snow" are not discarded and can create unrealistic high albedo values.

3.6 RISK OF FAILURE AND MITIGATION MEASURES

As the product depends on the BRDF inversion step in the TOC-r chain, any solution to continue the processing of the TOC-r products is a mitigation measure for the Surface Albedo product. As such, in case the PROBA-V sensor fails, or its quality is degraded, the METOP/AVHRR sensor could be envisioned to be used to continue the processing of SA products.

4 REFERENCES

- Bartholomé, E. and Belward, A.S., 2005. GLC2000: a new approach to global land cover mapping from Earth Observation data. *International Journal of Remote Sensing*, 26(9): 1959 - 1977.
- Carrer, D., Roujean, J.-L. & Meurey, C. Comparing operational MSG/SEVIRI land surface albedo products from Land SAF with ground measurements and MODIS. *IEEE Transactions on Geoscience and Remote Sensing* 48, 1714-1728 (2010).
- Dierckx, W., Sterckx, S., Benhadj, I., Livens, S., Duhoux, G., Van Achteren, T., Francois, M. Mellab, K. and G. Saint, 2014. PROBA-V mission for global vegetation monitoring: standard products and image quality. *Int. J. Remote Sens.*, vol. 35, issue 7, p. 2589-2614
- Diner D.J., Martonchik J.V., Borel C., Gerstl S.A.W., Gordon H.R., Knyazikhin Y., Myneni R., Pinty B., Verstraete M.M., 1999, MISR Level 2 Surface Retrieval Algorithm Theoretical Basis. *Jet Propulsion Laboratory D-11401, Rev. D*.
- Dozier, J., (1989). Spectral signature of alpine snow cover from Landsat 5 TM. *Remote Sensing of Environment*, 28: 9 - 22.
- GCOS, 2003: Second report on the adequacy of the global observing systems for climate. *Technical Report GCOS-82 (WMO/TD No 1143): World Meteorological Organization*.
- GCOS, 2006: Systematic observation requirements for satellite-based products for climate: Supplemental details to the satellite-based component of the implementation plan for the global observing system for climate in support of the UNFCCC. *Technical Report GCOS-107, WMO/TD No. 1338: World Meteorological Organization*.
- Fensholt, R., Rasmussen, K., Nielsen, T.T., Mbow, C., 2009. Evaluation of earth observation based long term vegetation trends - Intercomparing NDVI time series trend analysis consistency of Sahel from AVHRR GIMMS, Terra MODIS and SPOT VGT data. *Remote Sens. Environ.*
- François, M., S. Santandrea, K. Mellab, D. Vrancken, and J. Versluys (2014). The PROBA-V mission: The space segment. *Int. J. Remote Sensing*, 35, 2548 – 2564, doi:10.1080/01431161.2014.883098.
- Geiger, B., Carrer, D., Franchisteguy, L., Roujean, J.-L. & Meurey, C. Land surface albedo derived on a daily basis from Meteosat second generation observations. *IEEE Transactions on Geoscience and Remote Sensing* 46, 3841-3856 (2008).
- Govaerts, Y. M., et al., 2008, Generating global surface albedo products from multiple geostationary satellites, *Remote Sensing of Environment*, doi:10.1016/j.rse.2008.01.012.
- Hagolle O., Lobo A., Maisongrande P., Cabot F., Duchemin B., and de Pereyra A., 2004, *Quality assessment and improvement of temporally composited products of remotely sensed imagery by combination of VEGETATION 1 & 2 images*, *Remote Sensing of Environment*, 94, 172-186.

Hook S. J., 1998, ASTER Spectral Library. <http://speclib.jpl.nasa.gov>

- Hosgood B., Jacquemoud S., Andreoli G., Verdebout J., Pedrini G., Schmuck G., 1995, Leaf Optical Properties EXperiment 93 (LOPEX93). *European Commission, Joint Research Centre, Institute for Remote Sensing Applications, Report EUR 16095 EN.*
- Jacquemoud, S., Baret F., 1990, PROSPECT: a model of leaf optical properties spectra. *Remote Sensing of Environment*, 34, 75-91.
- Leroy M., Deuzé J.L., Bréon F.M., Hautecoeur O., Herman M., Buriez J.C., Tanré D., Bouffières S., Chazette P., and Roujean J.L., 1997, Retrieval of atmospheric properties and surface bidirectional reflectances over land from POLDER/ADEOS, *Journal of Geophysical Research*, 10, 17023-17037.
- Liang, S., 2000, Narrowband to broadband conversions of land surface albedo: I Algorithms. *Remote Sensing of Environment*, 76, 213-238.
- Liang S., 2003, A direct algorithm for estimating land surface albedos from MODIS imagery. *IEEE Transactions on Geoscience and Remote Sensing*, 41, 136-145.
- Lucht W. and Lewis P., 2000, Theoretical noise sensitivity of BRDF and albedo retrieval from the EOS-MODIS and MISR sensors with respect to angular sampling. *International Journal of Remote Sensing*, 21(1), 81-98.
- Martonchik, J. V., Diner, D. J., Pinty, B., Verstraete, M., Myneni, R. B., Knyazikhin, Y., et al., 1998, Determination of land and ocean reflective, radiative, and biophysical properties using multiangle imaging. *IEEE Transactions on Geoscience and Remote Sensing*, 36, 1266–1281.
- Pinty B., Roveda F., Verstraete M.M., Gobron N., Govaerts Y., Martonchik J.V., Diner D.J., and Kahn R.A., 2000, Surface albedo retrieval from Meteosat. *Journal of Geophysical Research*, 105(D14), 18099-18134.
- Roujean J.-L., Leroy M., Deschamps P.-Y., 1992, A bidirectional reflectance model of the Earth's surface for the correction of remote sensing data. *Journal of Geophysical Research*, 97(D18), 20455-20468.
- Samain O., 2006, Fusion multi-capteurs de données satellitaires optiques pour la restitution de variables biogéophysiques de surface, Ph. D. Université P. Sabatier Toulouse III.
- Schaaf, C. B., Gao, F., Strahler, A. H., Lucht, W., Li, X., Tsang, T., et al., 2002, First operational BRDF, albedo and nadir reflectance products from MODIS. *Remote Sensing of Environment*, 83, 135–148.
- Sterckx, S., Benhadj, I., Duhoux, G., Livens, S., Dierckx, W., Goor, E., Adriaensen, S., Heyns, W., Van Hoof, K., Strackx, G., Nackaerts, K., Reusen, I., Van Achteren, T., Dries, J., Van Roey, T., Mellab, K., Duca, R. and Zender, J. (2014). The PROBA-V mission: image processing and calibration. *Int. J. Remote Sens.*, 35(7), 2565 – 2588.
- Strahler A.H., Muller J.P. et al. (21 authors), 1999, MODIS BRDF/Albedo Product: Algorithm Theoretical Basis Document, version 5.0, 53 p.

Verhoef W., 1984, Light scattering by leaf layers with application to canopy reflectance modeling, the SAIL model. *Remote Sensing of Environment*, 16, 125-141.

ANNEX 1: COEFFICIENTS FOR ALBEDO CALCULATION

Table 7: Look-up table of directional-hemispherical and bi-hemispherical kernel integrals as a function of solar zenith angle for the Roujean et al. (1992) model.

θ_{in}	I_0^{dh}	I_1^{dh}	I_2^{dh}
0°	1.0	-0.997910	-0.00894619
5°	1.0	-0.998980	-0.00837790
10°	1.0	-1.00197	-0.00665391
15°	1.0	-1.00702	-0.00371872
20°	1.0	-1.01438	0.000524714
25°	1.0	-1.02443	0.00621877
30°	1.0	-1.03773	0.0135606
35°	1.0	-1.05501	0.0228129
40°	1.0	-1.07742	0.0343240
45°	1.0	-1.10665	0.0485505
50°	1.0	-1.14526	0.0661051
55°	1.0	-1.19740	0.0878086
60°	1.0	-1.27008	0.114795
65°	1.0	-1.37595	0.148698
70°	1.0	-1.54059	0.191944
75°	1.0	-1.82419	0.248471
80°	1.0	-2.40820	0.325351
85°	1.0	-4.20369	0.438371

θ_{in}	I_0^{bh}	I_1^{bh}	I_2^{bh}
0°-90°	1.0	-1.28159	0.0802838

ANNEX 2: NARROW-TO-BROADBAND CONVERSION COEFFICIENTS

Table 8: Narrow to broadband conversion coefficients for the SPOT/VEGETATION-2 channels.

Broadband	Cases	$C_{0\gamma}^{xh}$	$C_{1\gamma}^{xh}$ Blue	$C_{2\gamma}^{xh}$ Red	$C_{3\gamma}^{xh}$ NIR	$C_{4\gamma}^{xh}$ SWIR	σ [reg]
Visible	Snow	0.0284	0.57795	0.37077	-	-	0.0199
	Snow & B0 saturated	0.0255	-	0.89055	0.06964	-0.31278	0.0212
	Snow & (B0 and B2 saturated)	0.0792	-	-	1.01062	-1.82936	0.0685
	Other cases	0.0010	0.50791	0.47503	-	-	0.0067
Near-Infrared	Snow	0.0212	-	0.04437	0.55193	0.36701	0.0128
	Snow & B0 saturated	0.0236	-	-	0.59939	0.28744	0.0132
	Snow & (B0 and B2 saturated)	-	-	-	-	-	-
	Other cases	0.0140	-	0.00882	0.56868	0.35175	0.0135
Total	Snow	0.0248	0.12171	0.26775	0.35725	0.08221	0.0154
	Snow & B0 saturated	0.0266	-	0.39913	0.34290	0.05098	0.0157
	Snow & (B0 and B2 saturated)	0.0525	-	-	0.76376	-0.65405	0.0328
	Other cases	0.0097	0.18875	0.21475	0.34410	0.18457	0.0089

Table 9: Narrow to broadband conversion coefficients for the PROBA-V channels.

Broadband	Cases	$C_{0\gamma}^{xh}$	$C_{1\gamma}^{xh}$ Blue	$C_{2\gamma}^{xh}$ Red	$C_{3\gamma}^{xh}$ NIR	$C_{4\gamma}^{xh}$ SWIR	σ [reg]
Visible	Snow	0.0284	0.5736	0.3837	-	-	0.0199
	Snow & B0 saturated*	0.0255	-	0.89055	0.06964	-0.31278	0.0212
	Snow & (B0 and B2 saturated)*	0.0792	-	-	1.01062	-1.82936	0.0685
	Other cases	0.0010	0.5039	0.4923	-	-	0.0067
Near-Infrared	Snow	0.0212	-	0.0438	0.5509	0.3633	0.0128
	Snow & B0 saturated*	0.0236	-	-	0.59939	0.28744	0.0132
	Snow & (B0 and B2 saturated)	0.0236	-	-	0.59939	0.28744	0.0132
	Other cases	0.0140	-	0.0068	0.5677	0.3481	0.0135
Total	Snow	0.0248	0.1196	0.2764	0.3566	0.0789	0.0154
	Snow & B0 saturated*	0.0266	-	0.39913	0.34290	0.05098	0.0157
	Snow & (B0 and B2 saturated)*	0.0525	-	-	0.76376	-0.65405	0.0328
	Other cases	0.0097	0.1863	0.2212	0.3434	0.1817	0.0089

Note the cases with asterix (*) have the same coefficients as SPOT-VGT2 channels (Table 8).